Title:

IntelliProfiler: a novel analytic tool for behavior dynamics of multiple animals in a home cage

Authors: Shohei Ochi[1*], Hitoshi Inada[1,2], Noriko Osumi[1*]

Affiliation:

[1] Department of Developmental Neuroscience, Tohoku University Graduate School of Medicine, Sendai, Miyagi 980-8575, Japan

[2] Department of Biochemistry and Cellular Biology, National Institute of Neuroscience, NCNP, Kodaira, Tokyo, Japan.

*Correspondence: noriko.osumi.c7@tohoku.ac.jp and shohei.ochi.a5@tohoku.ac.jp

Abstract

There is a growing demand for sophisticated behavioral analysis systems that minimize bias in multi-animal and semi-natural environments. We present "IntelliProfiler," an advanced system using radio frequency identification (RFID) technology to enable fully automated behavior analyses of multiple mice within a home cage. IntelliProfiler continuously monitors up to 16 mice, capturing both locomotor activity and social dynamics over extended periods. Our findings revealed that male mice maintain broader social distances than females, with group size playing a key role in shaping male social network dynamics. Furthermore, aging in males significantly impacts both locomotor activity and social interaction in a group size-dependent manner. With its ability to provide in-depth analysis of individual and group behaviors, IntelliProfiler offers a novel approach for exploring complex social interactions and group dynamics, advancing the field of behavioral science.

Introduction

Behavioral analyses using model animals are crucial for understanding neural functions and pathological states. Due to its ease of handling and suitability for genetic manipulations, the laboratory mouse is widely used as a model animal to study neural bases of various conditions, including psychiatric, neurodevelopmental, and neurodegenerative disorders. Traditional methods for analyzing neural functions in mice involve assessing behaviors, such as locomotion, exploration, social interaction, and learning/memory through specific tests including the open field test, the elevated plus maze, the social interaction test, and the Morris water maze[1–4]. However, these traditional approaches come with several limitations.

A major limitation of traditional behavioral analyses is the low throughput of data acquisition, as most analyses are manually conducted over limited periods under artificial conditions. Typically, behavior is recorded for a single mouse in a specific experimental setup. For instance, the open field test measures general locomotor activity and anxiety-related behavior by placing a single mouse in an open arena and tracking its movements and time spent in different zones[1]. Similarly, the three-chamber social interaction test assesses sociability by comparing the time a mouse interacts with a

novel mouse versus an empty chamber, offering insights into social preferences[5]. A more significant concern, however, is that interactions between experimenters and animals often introduce biases that influence results[6–8]. Handling by experimenters can elevate heart rate, body temperature, spontaneous activity, and anxiety, potentially impacting memory and learning abilities[7,9]. Moreover, variations in behavioral data have been linked to the researcher's gender and environmental conditions[8,10]. Therefore, there is a growing need for automated, unbiased systems to analyze behavior in natural (home-caged) conditions to ensure more robust and reliable data.

Recent trends in behavioral analyses have shifted towards studying group dynamics in semi-natural environments. One prominent approach is the use of video tracking systems with computer visions, such as DeepLabCut (DLC)[11–13]. DLC leverages deep learning to achieve markerless pose estimation, offering high precision tracking with minimal training data[14]. Despite its accuracy, video tracking systems face limitations when tracking larger groups. Identifying individual animals becomes technically challenging due to issues like visual cue swapping or obscuring during group behaviors, such as huddling or fighting.

Another approach involves tracking systems using contactless tags, such as radio frequency identification (RFID) chips. IntelliCage, a pioneering RFID system, utilizes RFID readers placed at the corners of a cage to automatically monitor the frequency and timing of animals entering chambers[15]. IntelliCage has been widely used to investigate spontaneous behavior and learning in group-housed mice[16,17]. Another RFID-based system, ECO-HAB, consists of four open fields connected by tubes, with RFID readers positioned at the junctions, allowing the study of free movement and social interactions among mice by tracking their movement between fields[18,19]. More recently, RFID floor arrays have been developed to track multiple animals with higher time resolution[20]. While these RFID systems provide valuable insights into group behavior, they often lack the spatial or temporal resolution required for more detailed analyses.

In this study, we developed an innovative RFID-based behavioral analysis system, IntelliProfiler, to automatically monitor multiple mice in a home-cage environment. IntelliProfiler excels in its ability, accommodating groups ranging from four to 16 mice, while offering superior spatial and temporal resolution compared to existing systems. It enables long-term, continuous monitoring of both activity and sociability with minimal researcher intervention. Using IntelliProfiler, we conducted 72-hour continuous

behavioral analyses on large groups of male and female wild-type mice and compared behavioral patterns between sexes, as well as between young and aged male mice, to investigate the effects of aging on social dynamics. The insights gained through IntelliProfiler provide a deeper understanding of group behavior dynamics, advancing the precision and reliability of behavior research.

Results

Long-term activity measurement of group-housed mice

First, we set up our IntelliProfiler system using the antenna board comprising 96 antenna tiles arranged in a 12 x 8 grid (Fig. 1a). A large plastic cage (58 cm x 38 cm x 21.5 cm = width × depth × height) with a cage lid with food pellets, and three water bottles for long-term housing was placed on the antenna board (Fig. 1a, b). The IntelliProfiler software (see Methods) offers multiple functions: (1) data collection and preprocessing, (2) calculation of travel distance, relative distance between two mice, and spatial interaction proportion, (3) network analysis, (4) principal component analysis (PCA), and (5) figure visualization. Data including time, antenna ID, and transponder ID, were exported from the antenna board via Universal Serial Bus (USB) using TeraTerm software (Fig. 1c). In the data collection and preprocessing step, raw

102 data were converted into a per-second format with time, antenna ID, transponder ID,
103 and X-Y coordinates using initial function of IntelliProfiler software we developed (Fig.
104 1d, see Data collection and preprocessing in Method section). Further calculations,
105 analyses, and figure visualization were conducted using the converted data generated in
106 the data collection and preprocessing step (see Travel distance for each mouse, Relative
107 distance between two mice, Spatial interaction analysis, Close contact: defining social
108 proximity, Network Analysis, Principal component analysis, Figure visualization in
109 Method section). We conducted continuous 72-hour behavioral analyses on 8-week old
110 male and female mice with group sizes of four, eight, and 16 mice (Fig. 1e). Due to the
111 dislodging of one RFID tag in the group of 16 male mice, data from 15 male mice were
112 used for analysis, following the methodology of a previous article[21].
113
114 In the males, cumulative travel distances for every 2 hours exhibited the highest travel
115 distance values in the four-mouse group than the eight- and 15-mouse groups during
116 most of the time (Fig. 2a). The male mice exhibited the highest travel distance
117 immediately after entry, dropping by less than half within 2 hours (Fig. 2a). Their travel
118 distance increased again during the transition from light to dark period (Fig. 2a). In

119 contrast, females showed less active and stable travel distances across almost all time
120 points (Fig. 2b).
121
122 To understand the general trends of locomotor activity in the male and female mice, we
123 analyzed cumulative travel distances in 12-hour intervals (Fig. 2c, d). The males
124 showed the highest travel distance just after their entry and significantly higher travel
125 distance in the group of four mice than in the groups of eight and 15 mice (Fig. 2c).
126 Small but significant differences were observed between the eight- and 15-mouse
127 groups in the light period on day 1 and the dark period on day 3 (Fig. 2c). On the other
128 hand, females showed similar travel distances through the period among groups except
129 for day 1 (Fig. 2d).
130
131 To examine sex differences in locomotor activity within the same group size, we
132 compared 2-hour intervals activities in the groups of four, eight, and 15/16 mice (Fig.
133 2e-g). In the four-mouse group, male mice showed higher travel distances throughout
134 the period than females, with significantly higher travel distances observed at six time
135 points in the dark periods (Fig. 2e). However, no periodic trend was observed in eight-
136 and 15/16-mouse groups (Fig. 2f, g). In the cumulative travel distances in 12-hour

137 intervals (Fig. 2h-j), males showed higher travel distances throughout the period in the
138 four-mouse group than female mice except for the light period on day 3 (Fig. 2h). On
139 the other hand, no noticeable sex difference was observed in the groups of eight and
140 15/16 mice (Fig. 2i, j).
141
142 The time course of relative locomotor activity for each mouse was visualized as a
143 heatmap (Fig. 2k-n). Male mice showed a marked increase in activity immediately after
144 the introduction and at the onset of the dark period (Fig. 2k). A pronounced contrast of
145 locomotor activity was observed between light and dark periods over the course of 3
146 days (Fig. 2m). In contrast, female mice displayed relatively more variable activity
147 patterns over time (Fig. 2l), with some showing elevated activity even during the light
148 period (Fig. 2n). These findings suggest that male mice, particularly in smaller group
149 sizes, exhibit higher locomotor activity, pointing to potential sex-specific behavioral
150 responses to group size.
151
152 Social interactions between two individuals of group-housed mice
153 To assess social interactions among group-housed mice, we tracked changes in the
154 distance between two individual mice. The spatial relationships were classified into four

categories based on proximities: "Same" - the other mouse occupied the same grid as the focal mouse; "Close" - the other mouse was in the adjacent grids; "Intermediate" - the other mouse was located beyond the surrounding grids; and "Away" - the other mouse was farther than "Intermediate" (Fig. 3a). The transition in social distance ratios were recorded in 2-hour intervals for groups of four, eight, and 15 male mice (Fig. 3b-d) and for groups of four, eight, and 16 female mice (Fig. 3e-g).

The proportion of "Same" increased during the light period and decreased during the dark period in the four-mouse group, but this pattern was not observed in the other groups (Fig. 3b-g). A similar trend was found for the "Close" category, where its proportion rose in the light period and declined in the dark period across groups of four, eight, and 15 males, as well as four, eight, and 16 females (Fig. 3b-g). The proportion of "Intermediate" was relatively low in the four-mouse group but increased with group size, without showing a consistent periodic trend observed (Fig. 3b-g). In contrast, the proportion of "Away" decreased during the light period and increased in the dark period across all groups (Fig. 3b-g).

172 The average proportion of each social distance category during the light and dark
173 periods was compared across groups (Fig. 3b-g). The proportion of "Same" decreased as
174 group size increased (Fig. 3b-g). During the light period, the percentage of "Close" was
175 higher than during the dark period across all groups, though there was no clear trend
176 concerning group size (Fig. 3b-g). The proportion of "Intermediate" increased with
177 group size during the light period, and was higher in the groups of eight and 15/16 mice
178 than the four-mouse group during the dark period, but similar between the eight-mouse
179 and 15/16-mouse groups (Fig. 3b-g). In contrast, the proportion of "Away" was highest
180 in the 15-male group during both periods, although no clear pattern emerged for the
181 female groups. In summary, the "Same" category was more prevalent in the four-male
182 and four- or eight-female groups during the light period, but no consistent periodic trend
183 was found in the larger groups. Meanwhile, the proportion of "Away" was consistently
184 lower across all groups during the light periods (Fig. 3b-g). These analyses revealed
185 qualitatively distinct patterns of social distance in the eight- and 15/16-mouse groups
186 compared to the four-mouse group.
187
188 Significant differences in the proportions of each category between the light and dark
189 periods were observed in the groups of four males, as well as in the groups of four,

190 eight, and 16 females (Fig. 3b, e-g). However, no significant differences were found in
191 the groups of eight and 15 males (Fig. 3c, d). Regarding group size, significant
192 differences were noted in the male groups during both the light and dark periods, and in
193 the female groups during the light period (Fig. 3b-g), but no significant differences were
194 observed in the female groups during the dark period (Fig. 3e-g).
195
196 We then introduced the Close Contact Ratio (CCR), a metric to quantify social
197 proximity to analyze social interactions. This ratio reflects the proportion of time two
198 mice are either in the "Same" or "Close" (Fig. 4a). When CCR data were divided into 2-
199 hour intervals for both male and female groups (Fig. 4b, c), males in the four-mouse
200 group exhibited the highest CCR compared to the eight- and 15-mouse groups
201 throughout the entire period (Fig. 4b). In male mice, the CCR was initially low
202 immediately after entry, gradually increasing until 18:00, followed by a gradual decline
203 until 20:00, with a similar pattern recurring from day 2 onward (Fig. 4b). In contrast, the
204 females in the 16-mouse group showed a significantly lower CCR compared to the four-
205 and eight-mouse groups (Fig. 4c), although no consistent time-dependent pattern was
206 observed. We also analyzed the average CCR over 12-hour intervals (Fig. 4d, e). In
207 male mice, the CCR decreased as the group size increased from four to eight to 15 mice

208 during the light period (Fig. 4d). The 15-mouse group had the lowest CCR, while no
209 significant difference was found between the four- and eight-mouse groups during the
210 dark period (Fig. 4d). Similarly, female mice in the 16-mouse group tended to have the
211 lowest CCR during the light period compared to the four- and eight-mouse groups,
212 though no consistent differences were observed between the latter two groups (Fig. 4e).
213 No clear trend was observed during the dark period in female mice (Fig. 4e).
214
215 We also examined the sex differences in CCR using 2-hour intervals in four-, eight-,
216 and 15/16-mouse groups (Fig. 4f-h). In the four-mouse group, females showed a
217 significantly higher CCR during the initial 4 hours (Fig. 4f). However, CCR fluctuated
218 between males and females throughout the remaining time points, suggesting that
219 consistent sex differences in social proximity might not be present in this group (Fig.
220 4f). In contrast, in the eight- and 15/16-mouse groups, females consistently exhibited
221 higher CCR than males at most time points, indicating more pronounced sex differences
222 in social proximity (Fig. 4g, h). To assess overall trend, we analyzed the CCR in 12-
223 hour intervals (Fig. 4i-k). In the four-mouse group, no clear sex differences in CCR
224 were observed, except during the light period on day 2, when females had a higher CCR
225 (Fig. 4i). However, in the eight-mouse group, females had a higher CCR than males

226 across most periods, except during the dark period on day 3 (Fig. 4j). Similarly, in the
227 16-mouse group, females consistently exhibited a higher CCR than males across all the
228 periods (Fig. 4k).
229
230 The time course of CCR, visualized as a heatmap for individual mice (Fig. 4l-o),
231 revealed a strong periodic trend in the males, with CCRs peaking during the light period
232 and decreasing during the dark period (Fig. 4l). In contrast, the female groups generally
233 displayed higher CCRs for longer durations compared to males (Fig. 4l, m). The
234 periodic patterns of CCRs were less pronounced in the 15/16 mouse groups, though the
235 trend remained more apparent in males than females (Fig. 4l-o). These findings suggest
236 that sex-specific social dynamics become more prominent in larger groups.
237
238 Aging effect
239 Since aging has been reported to affect many behavioral aspects, including locomotor
240 activity and social interaction[22,23], we compared young (8-week-old) and aged (53-
241 week-old) male mice in groups of four and eight (Fig. 1e). Activity levels of the mice
242 were analyzed using methods as those in Fig. 2. Both young and aged males in the four-
243 mouse group generally had longer travel distances compared to those in the eight-mouse

244 group at most time points (Fig. 5a). Regarding the group effect, aged males in the four-
245 mouse group showed a longer travel distance immediately after their introduction and
246 after the next transition from the dark and light period than those in the eight-mouse
247 group (Fig. 5b). Regarding the age effect, there was no significant difference in travel
248 distance between the young and aged males (Fig. 5c). In contrast, the aged male mice in
249 the eight-mouse group had consistently longer travel distances at almost all time points
250 compared to young male mice (Fig. 5d). The differences between young and aged mice
251 in the eight-mouse group was also significant than other comparison between aged mice
252 in the four- and eight-mouse groups as well as between young and aged mice in the
253 four-mouse group (Fig. 5e-g).
254
255 In the heatmap analysis, activity was also prominent immediately after the introduction
256 and at the onset of the dark period in all groups, although aged mice in the eight-mouse
257 group showed more activity throughout the period (Fig. 5h, i). In the heatmap of
258 cumulative activity over 12-hour intervals, aged males exhibited more diverse and
259 desynchronized activity, particularly in the eight-mouse group (Fig. 5j, k). Therefore,
260 the spontaneous activity was different between young and aged mice.
261

262 Next, we examined the changes in spatial relationships among young and aged male
263 mice in the four- and eight-mouse groups (Fig. 6a), similar to those in Fig. 3. Regarding
264 group effects, aged mice in the four-mouse group exhibited lower percentage of "Same"
265 category during the light and dark periods compared to young mice in the four-mouse
266 group, while aged mice in the eight-mouse group showed lower percentage of "Away"
267 in both periods compared to younger counterparts (Fig. 6b-e). In contrast, aged mice in
268 both the four- and eight-mouse groups consistently exhibited higher percentage of
269 "Intermediate" during both periods compared to young mice (Fig. 6b-e). These analyses
270 revealed distinct social proximity patterns in aged male mice compared to young male
271 mice, especially in the increased proportion of "Intermediate" in the aged groups.
272
273 We then analyzed CCRs in 2-hour intervals for both young and aged male mice in the
274 four- and eight-mouse groups (Fig. 7a), using methods similar to those in Fig. 4. Young
275 males in the four-mouse group exhibited a higher CCR than those in the eight-mouse
276 group at most time points (Fig. 7b). In contrast, aged males in the four-mouse group
277 displayed a higher CCR from 18:00-20:00 on day 2 compared to those in the eight-
278 mouse group (Fig. 7c). Regarding the age effect, aged mice in the four-mouse group
279 consistently showed a lower CCR during the light period at nearly all time points

280 compared to young mice in the four-mouse group (Fig. 7d). On the other hand, aged
281 mice in the eight-mouse group displayed non-consistent periodic trends, with lower
282 CCR amplitude of the light-dark cycle, compared to young mice in the eight-mouse
283 group (Fig. 7e). The CCR differences between young and aged mice in the four-mouse
284 group during the light period was also consistently more significant than those in the
285 comparisons between aged mice in the four- and eight-mouse groups, as well as
286 between young and aged mice in the eight-mouse group (Fig. 7f-h). In the heatmap
287 analysis, the young mice exhibited robust periodic trends, with elevated CCR values
288 during the light period and decreased values during the dark period, particularly in the
289 four-mouse group (Fig. 7i). In contrast, the aged mice in both the four- and eight-mouse
290 groups showed more stable, intermediate CCR values compared to young mice (Fig. 7j).
291 In the heatmap of cumulative activity over 12-hour intervals, aged males demonstrated
292 more ambiguous cyclic CCR patterns, particularly in the eight-mouse group (Fig. 7k, l).
293 These findings suggest that aging in male mice altered not only locomotor activity but
294 also the temporal dynamics of social behaviors.
295
296 Characterization of group behaviors

297 To investigate the behavioral characteristics of each group, we conducted principal
298 component analysis (PCA) using four key parameters. First, we defined normalized
299 activity as the activity at time *t*, divided by the maximum activity value recorded over
300 Days 1-3, and multiplied by 100 to standardize the data. This allowed us to calculate the
301 normalized activity in both the light (AL) and dark (AD) periods by averaging activity
302 values at each time point over three days. We selected four parameters for PCA:
303 sociability, measured as CCR values during the light (SL) and dark (SD) periods
304 (parameters 1 and 2, respectively), and normalized activity during the light (AL) and
305 dark (AD) periods (parameters 3 and 4, respectively). Correlations among these
306 parameters are shown in Supplementary Fig. 1, 2, while the PCA results with estimated
307 clusters are displayed in Fig. 8. The number of clusters was determined using the Elbow
308 method[24] and further assessed through Silhouette plots[25] (Supplementary Fig. 3).
309 The PCA revealed distinct sex-biased groupings. Notably, the male mice in the 15-
310 mouse group formed a well-defined separated cluster, whereas the male and female
311 mice in the four-mouse groups and female mice in the eight-mouse group clustered
312 together (Fig. 8a). Interestingly, female mice in the 16-mouse group split into two
313 clusters, with one cluster aligning with the male mice in the eight-mouse group (Fig.
314 8b). This suggests that while smaller groups tend to blend, significant sex differences

emerge in larger groups. In the feature space, AL and AD vectors pointed in the same direction, indicating similar patterns of activity, while SL and SD vectors diverged, reflecting different sociability dynamics between light and dark periods (Fig. 8c). In terms of aging effects, young and aged mice in the four-mouse groups were largely positioned in the positive X and Y directions, whereas those in the eight-mouse groups clustered near the origin (0,0) or in the negative X direction (Fig. 8d). K-means clustering effectively separated the four- and eight-mouse groups (Fig. 8e), and each feature vector had a distinct direction (Fig. 8f), indicating that aging influenced both activity and sociability in distinct ways, aligning with our earlier observations (Fig. 5-7).

Network analysis of social interactions

We explored how group size influences social interaction networks (Fig. 9). Qualitatively, there was no noticeable difference in network structure between male and female mice in the four- and eight-mouse groups (Fig. 9). However, in the 15/16-mouse groups, male mice exhibited increased social proximity and developed more expanded networks, influenced by light-dark circadian rhythms. In contrast, female mice maintained relatively uniform network structures (Fig. 9). When comparing young and

333 aged male mice in the four-mouse groups, no significant differences in network
334 structure were observed (Fig. 10). In the eight-mouse groups, however, young male
335 mice displayed increased social proximity and formed diverse networks that fluctuated
336 with light-dark cycles, while aged male mice maintained more stable, uniform networks
337 with only slight variation corresponding to circadian rhythms (Fig. 10*)*. These findings
338 suggest that male and female mice create distinct social environments, and that aging
339 may impact the complexity and heterogeneity of the networks in larger groups.
340

341 Analysis of individual social interactions

342 Lastly, we focused on individual differences in social interactions through a pairwise
343 analysis of CCR. In the heatmap presentations (Supplementary Fig. 6), no obvious
344 individual differences were observed between sexes in the four- and eight-mouse
345 groups. However, in the 15/16-mouse groups, two males (mouse ID #1 and #2)
346 exhibited lower CCR scores compared to the others, while all female mice showed
347 similar CCR patterns. Additionally, male mice tended to display higher CCR during the
348 light period, which decreased during the dark period, whereas female mice maintained
349 relatively stable CCR levels with less fluctuation across the light and dark periods,
350 indicating a sex-dependent response to light. Regarding the aging effect, aged males

showed lower CCR scores and more ambiguous, less defined time-dependent patterns compared to young males (Supplementary Fig. 7), consistent with mean values presented in Fig. 7. These findings suggest that individuality may develop progressively with aging in males, potentially contributing to the observed social dynamics.

356 **Discussion**

357 In this study, we developed a novel RFID-based behavioral analysis system,
358 IntelliProfiler, which allows for continuous, unbiased monitoring of up to 16 mice
359 within the home-cage environment. This system has provided clear insights into the
360 effects of group size, sex, and aging on both locomotor activity and social interactions,
361 offering a more comprehensive understanding of the semi-natural behaviors of group-
362 housed mice than using traditional behavioral methods can achieve.

363

364 One of our key findings was the impact of group size on behavior. IntelliProfiler
365 revealed significant differences in activity levels and social proximity, particularly
366 among males, where larger groups reduced activity. Traditional behavior paradigms,
367 such as the open-field test, are typically designed for individual animals[26,27], and
368 therefore fail to capture the complexities of behavior in group settings. These
369 conventional paradigms may overlook critical dynamics unique to multi-animal
370 environments. A recent article in *Nature Digest* emphasized the importance of studying
371 animals under 'natural conditions' to gain deeper insights into their behavior[28].
372 IntelliProfiler enables us to monitor authentic locomotor activity under semi-natural

373 conditions, offering a more comprehensive understanding of how group size shapes
374 individual activity and social dynamics.
375
376 In this study, we introduced CCR as a novel social parameter to measure social
377 proximity, representing a significant advancement in behavioral analysis (Fig. 4).
378 Traditional social interaction tests, such as the three-chamber test, offer limited insight
379 into short-term interactions, but the CCR provides a more detailed, long-term view of
380 group dynamics. Notably, we found that females tended to form stable clusters, while
381 males exhibited more fluid, group size-dependent social patterns (Fig. 4, 8, 9). This
382 underscores IntelliProfiler's ability to detect subtle, yet important sex-specific social
383 behaviors, often overlooked by conventional methods.
384
385 Aging also influenced locomotor activity and social interactions, with aged males
386 displaying less distinct and more variable CCR patterns compared to young males. This
387 finding aligns with previous research on aging and social behavior,[23,29] but also suggests
388 that IntelliProfiler offers a more nuanced understanding of how aging affects social
389 dynamics, especially in larger groups (Fig. 7).
390

391 IntelliProfiler further provides an inexpensive, high-throughput platform for social
392 network analysis, surpassing the limitations of human observation. Although sexual
393 interaction between males and females is beyond our current purpose, our system would
394 be applicable to analyze sexual or courtship behaviors in large groups. While video
395 tracking systems have been useful for analyzing small groups, IntelliProfiler extends
396 this capability to larger groups, making it a crucial tool for studying population-level
397 behaviors.
398
399 Despite its advantages, IntelliProfiler has a few limitations. First, its spatial resolution is
400 lower than video-based tracking systems like DLC[11,30], as the current grid size is 5 cm x
401 5 cm, allowing two mice located in parallel. Additionally, determining body orientation
402 is challenging when the animal remains within the same grid. Second, the system has
403 difficulty distinguishing detailed social contacts, such as sniffing, mounting, or
404 huddling. Lastly, the current RFID system requires surgery for transponder
405 implantation, and it is not yet possible to eliminate the invasive effects due to the size of
406 commercially available transponders. These challenges should be addressed in future
407 developments.
408

Conclusion

The IntelliProfiler makes a significant advancement in animal behavior research, enabling continuous, detailed, and unbiased monitoring of individual movements and interactions within dynamic and complex social environments. Our findings highlight the critical roles of group size, sex, and aging in shaping behavior. This system provides a powerful tool for studying behavior in more naturalistic settings, offering new avenues for large-scale behavioral research and deeper insights into social dynamics.

418 **Methods**

419 Animals

420 C57BL/6J mice at 7- or 52-week old were purchased from CLEA Japan, Inc., and

421 maintained in the animal facility at Tohoku University Graduate School of Medicine.

422 An RFID tag (7 mm x 1.25 mm, Phenovance LCC) was subcutaneously implanted into

423 the abdomen of each mouse under anesthesia using 2.0% isoflurane (MSD Japan). The

424 mice were recovered for 1 week before starting behavioral recording. The recordings

425 started at 8- or 53-week old. All experimental procedures were approved by the Ethics

426 Committee for Animal Experiments at the Tohoku University Graduate School of

427 Medicine (approval number: 2021MdA-020-13).

428

429 Hardware

430 The antenaboard, comprising 96 antenna tiles arranged in 12x8 grids (5 cm by 5 cm

431 each) (Fig. 1a), was purchased from Phenovance LCC, Japan. The home cage used for

432 the study was 2000P cage (58 cm x 38 cm x 21.5 cm = width × depth × height,

433 Tecniplast, Italy), equipped with a cage lid with food pellets, and three water bottles for

434 long-term housing (Fig. 1a, b). Both the antenaboard and home cage were placed inside

435 a soundproof box (Phenovance LCC). The light-dark cycle in the soundproof box and

436 testing room was 12:12 hours (08:00-20:00, light; 20:00-08:00, dark). Mice were

437 introduced at 8:00 in the light period on day 1.

438

439 ## Software

440 R language (Version 4.2.2) was mainly used for preprocessing, data analysis, and

441 visualization[31]. Python (Version 3.9.7), Prism 9, and Microsoft Excel (Version 16.86)

442 were also used for preprocessing, data analysis, and visualization. R and Python

443 packages required for the scripts are listed in Supplementary Table 1.

444

445 ## Data collection and preprocessing

446 Data including time, antenna ID, and transponder ID, were exported from the

447 antenabord via Universal Serial Bus (USB) using TeraTerm software (Fig. 1c). The raw

448 data were converted into a format per second with time, antenna ID, transponder ID,

449 and X-Y coordinates (Fig. 1d). Missing values were interpolated by the immediately

450 preceding value.

451

452 ## Travel distance for each mouse

The Euclidean distances of mouse movement were calculated from consecutive RFID positions at time t and t+1. This was pivotal in understanding the spatial dynamics of the subjects. Graphical representations of tracked movements, including 2D positional plots and time series plots of X and Y coordinates, were generated to visualize trajectories and movement patterns over time.

Relative distance between two mice

The distances between different pairs of mice were calculated from the Euclidean distance between RFID positions. The total travel distance for each mouse was also calculated and plotted over the experimental period, providing a quantitative measure of activity levels.

Spatial interaction analysis

Spatial relationships of paired mice on the XY plane of the IntelliProfiler were classified, based on the distance L between the paired mice, into four categories (Fig. 3a). “Same” indicates that two mice were in the same grid (L=0 (cm)), suggesting immediate proximity. “Close” represents two mice were in adjacent grids (L=5 or $5\sqrt{2}$ (cm)), demonstrating close but distinct positions. “Intermediate” (L=10, $5\sqrt{5}$ or $10\sqrt{2}$

471 (cm)) places one mouse on the outer perimeter of "Close," while "Away" ($L>10\sqrt{2}$

472 (cm)) signifies that one mouse was outside of the range of "Intermediate," indicating

473 highly separation.

474

475 Close contact: defining social proximity

476 To examine social interactions within a group of mice, we defined the Close Contact

477 Ratio (CCR) as the cumulative percentage of time a pair of mice spent in the same grid

478 (defined as "Same") or adjacent grids (defined as "Close"). This measure serves as a

479 quantitative score of sociality between two mice, indicating their tendency to remain in

480 immediate or proximity. Utilizing Excel and Prism 9 (GraphPad Software), we

481 calculated the proportionate shifts of social distances ("Same," "Close," "Intermediate,"

482 and "Away") and CCR every 2 hours and in light and dark periods.

483

484 Network Analysis

485 Using Cytoscape 3.9.1[32], we conducted network analyses for four-, eight-, and 15/16-

486 mouse groups. We imported values ten times the CCR as edge betweenness into

487 Cytoscape 3.9.1. The network layout was generated using the Edge-weighted Spring

488 Embedded Layout, facilitating the visual interpretation of social interactions among the
489 mice based on their proximity metrics[32,33].
490

491 ## Principal component analysis

492 Principal component analysis (PCA) was conducted using Python 3 (Version 3.9.7) on
493 four datasets derived from long-term behavior mice in large groups under light and dark
494 periods, focusing on relative activity levels and CCR. Three distinct types of PCA plots
495 were generated: 1) PCA contribution vectors displayed on the PCA plot; 2) K-means
496 clustering analysis, with the optimal number of clusters determined using the elbow
497 method[24] and silhouette method[25] applied to the PCA plot; and 3) PCA plots color-
498 coded by gender and genotype to distinguish different groups.
499

500 ## Figure visualization

501 Graphical representations were primarily created using Prism 9 (GraphPad Software).
502 Time series line graphs and heat maps of travel distances or cumulative CCRs as well as
503 transitions in the proportionate of social distances ("Same," "Close," "Intermediate,"
504 and "Away") were visualized. Pie charts illustrating the distribution across social

505 distances were also developed. The PCA plots were designed in Python 3, and the social

506 network graphs for the groups were constructed using Cytoscape version 3.9.1.

507

508 Statistical analysis

509 Statistical analyses were performed with Prism version 9 (GraphPad). Two-way

510 ANOVA followed by Holm-Sidak's multiple comparisons test was applied to assess

511 differences between the two groups, which has been presented in part in a previous

512 article[34]. Values in the bar or line graphs were presented as mean ± SD, and $p^* < 0.05$,

513 $p^{**}<0.01$, $p^{***}<0.001$ indicated statistically significant differences. The p-values, F

514 values and degrees of freedom for all results, are provided in Supplementary Table 2.

515 All experiments were performed in a single repetition.

516

517 **Data availability**

518 The behavioral data generated in this study are provided in Supplementary Information.

519

520 **Code availability**

All code and scripts used for data analysis in this study are available on GitHub. To access the public repository, please use the following access token along with the repository URL:

- Repository URL: https://github.com/ShoheiOchi/IntelliProfiler

References

1. Hall, C. S. Emotional behavior in the rat. I. Defecation and urination as measures of individual differences in emotionality. *J Comp Psychol* **18**, 385–403 (1934).
2. Pellow, S., Chopin, P., File, S. E. & Briley, M. Validation of open:closed arm entries in an elevated plus-maze as a measure of anxiety in the rat. *J Neurosci Methods* **14**, 149–167 (1985).
3. File, S. E. & Hyde, J. R. Can social interaction be used to measure anxiety? *Br. J. Pharmac* **62**, 19–24 (1978).
4. Morris, R. Developments of a water-maze procedure for studying spatial learning in the rat. *J Neurosci Methods.* **11**, 47–60 (1984).
5. Moy, S. S. *et al.* Sociability and preference for social novelty in five inbred strains: an approach to assess autistic-like behavior in mice. *Genes Brain Behav* **3**, 287–302 (2004).
6. Balcombe, J. P., Barnard, N. D. & Sandusky, C. Laboratory routines cause animal stress. *Contemp Top Lab Anim Sci* **43**, 42–51 (2004).

542 7. Gouveia, K. & Hurst, J. L. Optimising reliability of mouse performance in
543 behavioural testing: The major role of non-aversive handling. *Sci Rep* **7:44999**,
544 (2017).
545 8. Georgiou, P. *et al.* Experimenters' sex modulates mouse behaviors and neural
546 responses to ketamine via corticotropin releasing factor. *Nat Neurosci* **25**, 1191–
547 1200 (2022).
548 9. Hurst, J. L. & West, R. S. Taming anxiety in laboratory mice. *Nat Methods* **7**,
549 825–826 (2010).
550 10. Sorge, R. E. *et al.* Olfactory exposure to males, including men, causes stress and
551 related analgesia in rodents. *Nat Methods* **11**, 629–632 (2014).
552 11. Mathis, A. *et al.* DeepLabCut: markerless pose estimation of user-defined body
553 parts with deep learning. *Nat Neurosci* **21**, 1281–1289 (2018).
554 12. de Chaumont, F. *et al.* Real-time analysis of the behaviour of groups of mice via
555 a depth-sensing camera and machine learning. *Nat Biomed Eng* **3**, 930–942
556 (2019).
557 13. Hakataya, S., Katsu, N., Okanoya, K. & Toya, G. An exploratory study of
558 behavioral traits and the establishment of social relationships in female
559 laboratory rats. *PLoS One* **18**, (2023).

14. Ye, S. *et al.* SuperAnimal pretrained pose estimation models for behavioral analysis. *Nat Commun* **15**, (2024).

15. Lipp, H.-P. High-throughput and automated behavioural screening of normal and genetically modified mice. *Business Briefing: Future Drug Discovery* 1–5 (2005).

16. Endo, T. *et al.* Automated test of behavioral flexibility in mice using a behavioral sequencing task in IntelliCage. *Behavioural Brain Research* **221**, 172–181 (2011).

17. Kiryk, A. *et al.* IntelliCage as a tool for measuring mouse behavior – 20 years perspective. *Behavioural Brain Research* **388**, (2020).

18. Chen, X. *et al.* Modelling collective behavior in groups of mice housed under semi-naturalistic conditions. *bioRxiv* (2024) doi:10.1101/2023.07.26.550619.

19. Winiarski, M. *et al.* Social deficits in BTBR T+ Itpr3tf/J mice vary with ecological validity of the test. *Genes Brain Behav* **21**, (2022).

20. Lipp, H. P. *et al.* IntelliCage: the development and perspectives of a mouse- and user-friendly automated behavioral test system. *Front Behav Neurosci* **17**, (2024).

21. Smutek, M. *et al.* A model of alcohol drinking under an intermittent access schedule using group-housed mice. *PLoS One* **9**, (2014).

22. Yanai, S. & Endo, S. Functional Aging in Male C57BL/6J Mice Across the Life-Span: A Systematic Behavioral Analysis of Motor, Emotional, and Memory Function to Define an Aging Phenotype. *Front Aging Neurosci* **13**, (2021).

23. Shoji, H., Takao, K., Hattori, S. & Miyakawa, T. Age-related changes in behavior in C57BL/6J mice from young adulthood to middle age. *Mol Brain* **9**, (2016).

24. Thorndike, R. L. Who belongs in the family? *Psychometrika* **18**, 267–276 (1953).

25. Rousseeuw, P. J. Silhouettes: A graphical aid to the interpretation and validation of cluster analysis. *J Comput Appl Math* **20**, 53–65 (1987).

26. Yoshizaki, K. *et al.* Paternal aging affects behavior in Pax6 mutant mice: A gene/environment interaction in understanding neurodevelopmental disorders. *PLoS One* **11**, (2016).

27. Crawley, J. N. Exploratory behavior models of anxiety in mice. *Neurosci Biobehav Rev* **9**, 37–44 (1985).

28. Smith, K. Lab mice go wild: making experiments more natural in order to decode the brain. *Nature* **618**, 448–450 (2023).

595 29. Shoji, H. & Miyakawa, T. Age-related behavioral changes from young to old age
596 in male mice of a C57BL/6J strain maintained under a genetic stability program.
597 *Neuropsychopharmacol Rep* **39**, 100–118 (2019).
598 30. Lauer, J. *et al.* Multi-animal pose estimation, identification and tracking with
599 DeepLabCut. *Nat Methods* **19**, 496–504 (2022).
600 31. R Core Team. R: A Language and Environment for Statistical Computing. R
601 Foundation for Statistical Computing, Vienna. (2021).
602 32. Shannon, P. *et al.* Cytoscape: A software Environment for integrated models of
603 biomolecular interaction networks. *Genome Res* **13**, 2498–2504 (2003).
604 33. Otasek, D., Morris, J. H., Bouças, J., Pico, A. R. & Demchak, B. Cytoscape
605 Automation: Empowering workflow-based network analysis. *Genome Biol* **20**,
606 (2019).
607 34. Endo, N. *et al.* The effects of maternal separation on behaviours under social-
608 housing environments in adult male C57BL/6 mice. *Sci Rep* **11**, (2021).
609
610

Acknowledgements

The authors are grateful to K. Tsutsui for temporally providing the behavioral analysis environment, and K. Abe for advising on the setup of the behavioral analysis room, and T. Endo for technical advice on constructing the antenaboard hardware. This research was funded by the JSPS KAKENHI (Grant-in-Aid for Transformative Research Areas) under grant number 24H01419 (to S.O.), AMED under grant number JP21wm0425003 (to N.O.). Takeda Science Foundation (to S.O.) and FY2024 Tohoku University Graduate School of Medicine Grant-in-Aid for Joint Research by Young Researchers (to S.O.).

Contributions

Conceptualization, S.O., H.I. and N.O.; behavior analysis, S.O.; data process, S.O. and H.I.; code preparation, S.O. and H.I.; figure preparation, S.O.; writing—review and editing, S.O., H.I. and N.O.; supervision, N.O.; project administration, S.O. and N.O.; funding acquisition, S.O., and N.O. All authors have read and agreed to the published version of the manuscript.

Competing interests

The authors declare that this study was conducted in the absence of any commercial or financial relationships that could be construed as a potential conflict of interest.

632 **Figures**

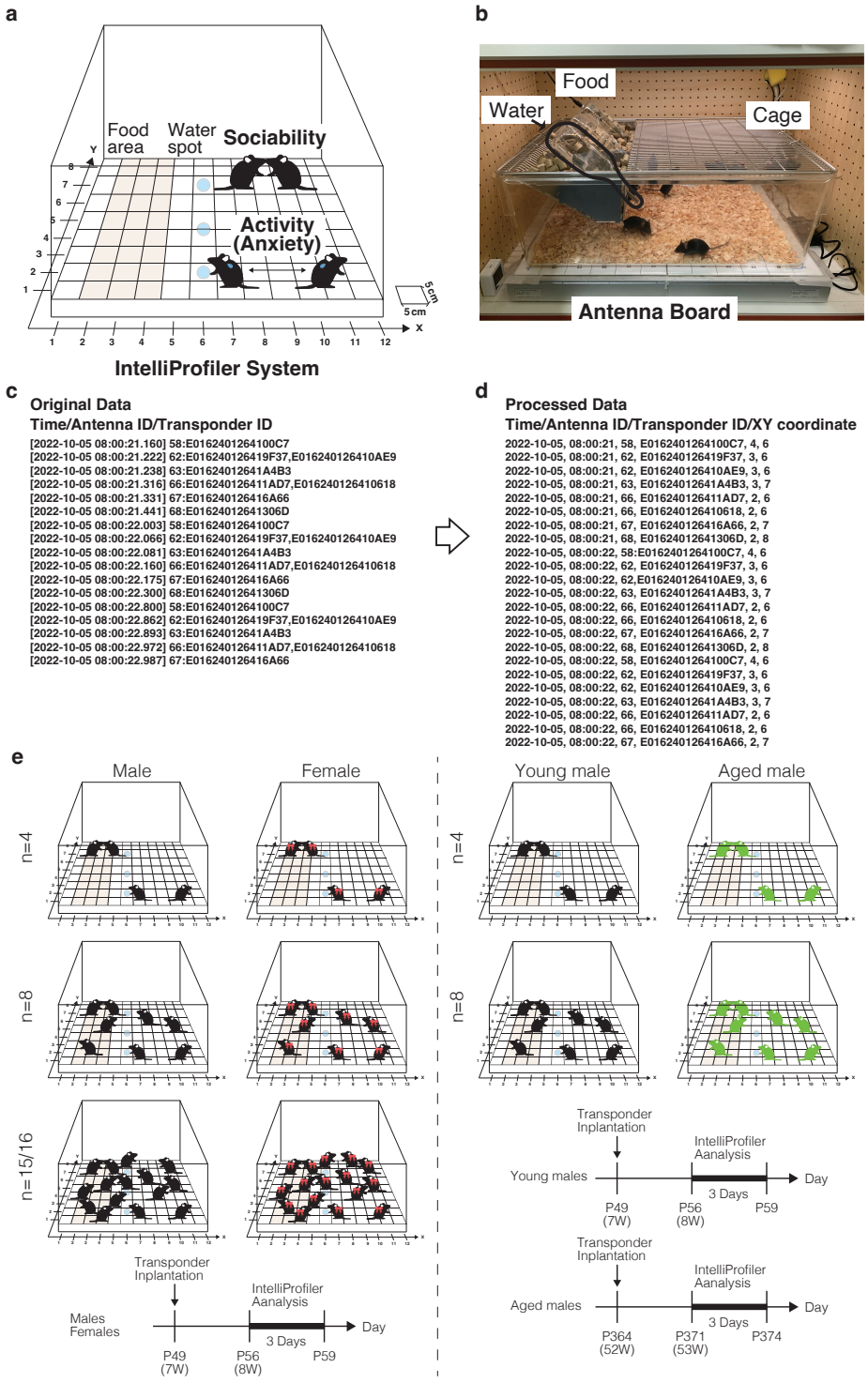

633

634 **Fig. 1: IntelliProfiler automated behavioral measurement system.**

a Schematic of the IntelliProfiler. The system tracks the location of mice implanted with RFID tags via detectors placed in a 96-grid array at the base, with each grid measuring 5 cm x 5 cm. Location information is converted into XY coordinates (X=12, Y=8), based on antenna IDs (1-96). **b** Photograph of the IntelliProfiler. **c** Original data, capturing information on Time, Antenna ID, and Transponder ID. **d** Processed data converted for the IntelliProfiler. The data is refined to includ Time, Antenna ID, Transponder ID, and XY coordinates. Decimal information is removed from the time data. Iif multiple individuals are detected on the same antenna ID simultaneously, their information is separated into different rows. **e** Behaior analysis was conducted over a continuous 72-hour period for male and female mice in groups of four-, eight- and 15/16. Additionally, young (8-week old) and aged (53-week old) male mice were analyzed in groups of four and eight.

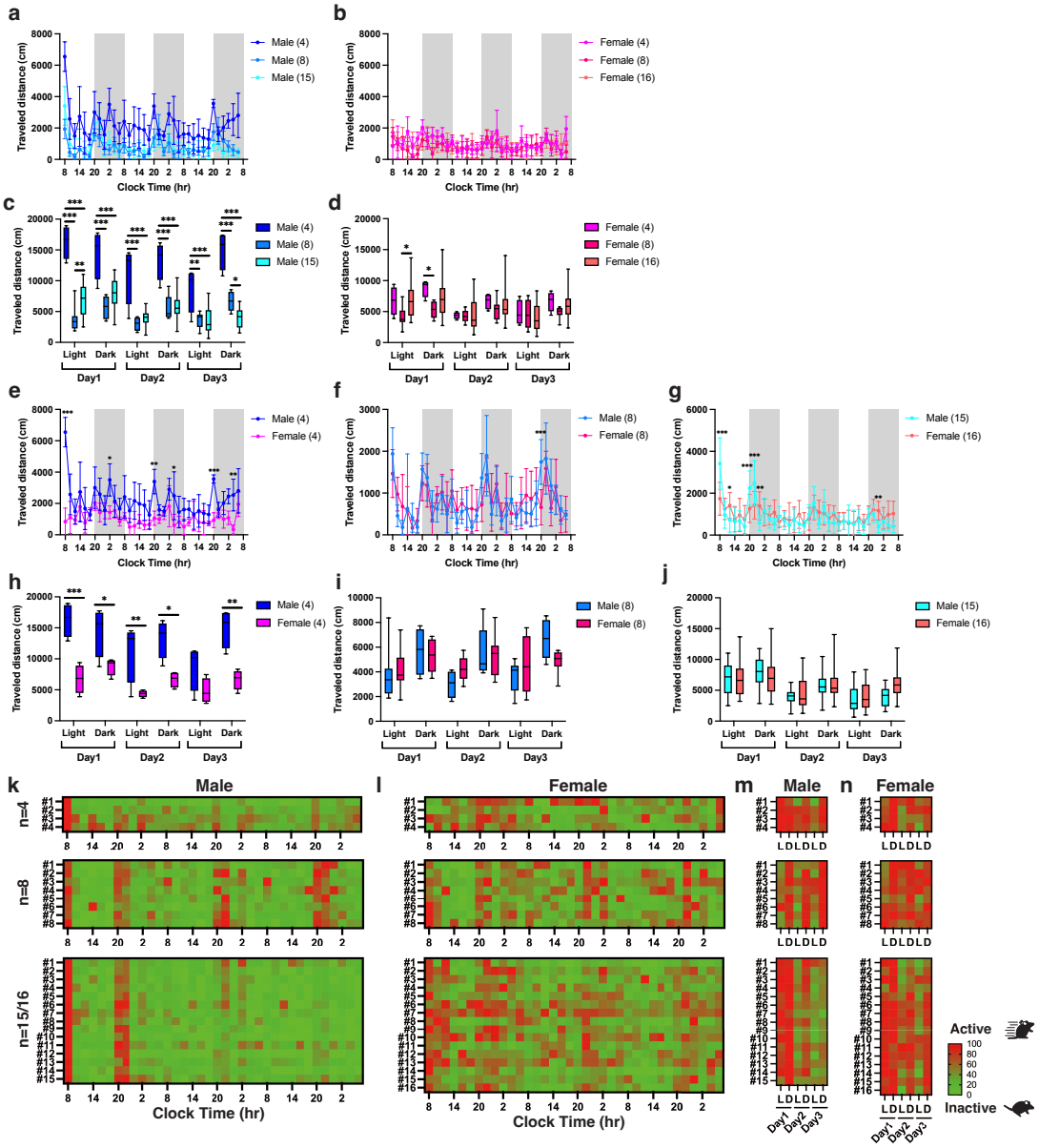

Fig. 2: Activity analysis of group-housed mice using the IntelliProfiler.

a-j Cumulative travel distances measured in 2-hour intervals (**a, b, e-g**) and over 12-hour intervals (light-dark cycles) (**c, d, h-j**). **a-d** Analysis of locomotor activity based on group size, comparing groups of four, eight, and 15 males (**a, c**) and four, eight, and 16 female mice (**b, d**). **e-j** Analysis of sex differences in locomotor activity, comparing groups of four (**e, h**), eight (**f, i**) and 15-16 (**g, j**) male and female mice. **k-n** Heatmaps showing relative locomotor activity over 2-hour intervals (**k, l**) and 12-hour intervals (**m, n**) for groups of four, eight, and 15-16 mice. Values in the bar or line graphs are presented as mean ± SD, with box plots displaying min/max whiskers. Statistical analysis was conducted using Holm-Sidak method for multiple comparison. Significance levels are indicated as $*p < 0.05$, $**p < 0.01$, and $***p < 0.001$. $p < 0.001$ (**c**), $p = 0.011$ (**d**), $p < 0.001$ (**e**), $p = 0.894$ (**f**), $p = 0.009$ (**g**), $p < 0.001$ (**h**), $p = 0.920$ (**i**), $p = 0.139$ (**j**).

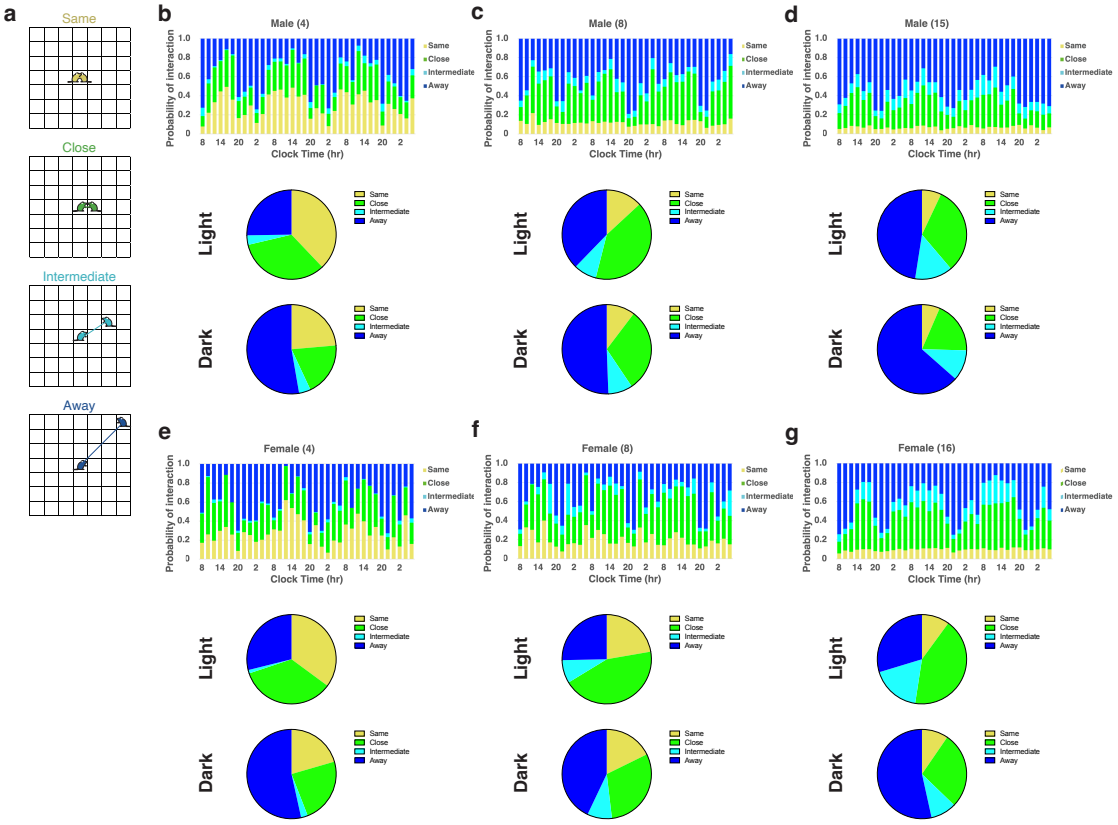

Fig. 3: The spatial relationships among group-housed mice using the IntelliProfiler.

a Definition of the spatial relationships between two individual mice. When another mouse is in the same grid as the focal mouse (both depicted in yellow), the relationship is defined as "Same." If the other mouse is in the surrounding grids (depicted in green), it is defined as "Close." If the other mouse is outside the surrounding grids (depicted in light blue), it is defined as "Intermediate." If the other mouse is beyond the "Intermediate" zone (depicted in blue), the relationship is categorized as "Away." **b-g** The 2-hour bin transition of proportions based on "Same," "Close," "Intermediate," and "Away" for groups of four male mice (**b**), eight male mice (**c**), 15 male mice (**d**), four female mice (**e**), eight female mice (**f**), and 16 female mice (**g**). The average proportion of distance categories during the light period and the dark period is shown for each group. Chi-square *p*-values comparing the proportions between light and dark periods: $p < 0.001$ (**b**, four males), $p = 0.256$ (**c**, eight males), $p = 0.114$ (**d**, 15 males), $p = 0.005$ (**e**, four females), $p = 0.049$ (**f,** eight females), $p = 0.007$ (**g**, 16 females). The *p*-values of chi-square for the group size, $p < 0.001$ (**b-d**, males in the light phase), $p = 0.002$ (**b-d**, males in the dark phase), $p < 0.001$ (**e-g**, females in the light phase), $p = 0.092$ (**e-g**, females in the dark phase).

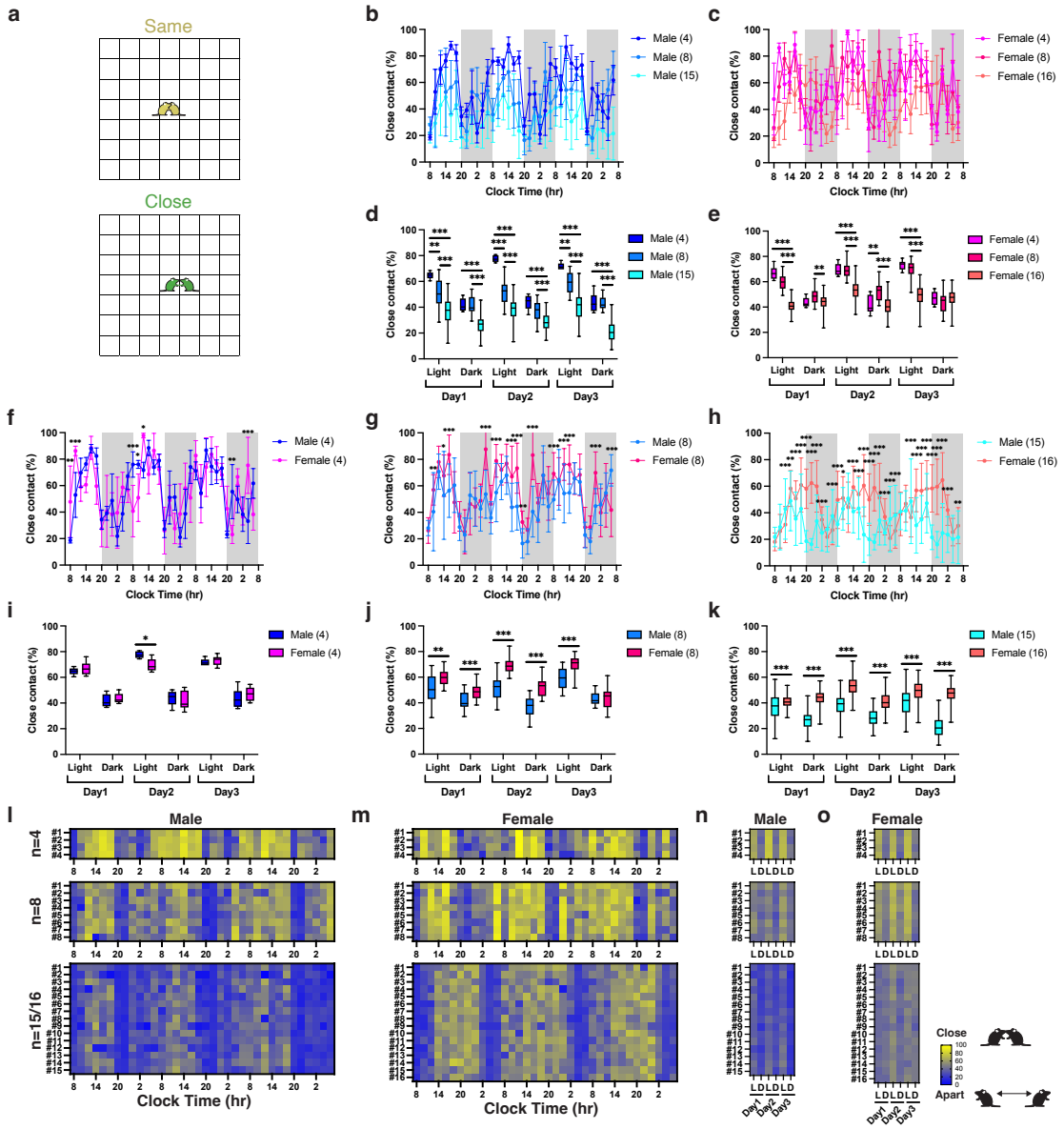

Fig. 4: Close contact between two individuals among group-housed mice analyzed using the IntelliProfiler.

686 **a** Definition of close contact, where two mice either in the "Same" grid (depicted in
687 yellow) or in adjacent grids, classified as "Close" (depicted in green). **b-k** Average
688 Close Contact Ratio (CCR) measured in in 2-hour intervals (**b, c, f-h**) and 12-hour
689 intervals (**d, e, i-k**). **b-e** Analysis of CCR based on group size, comparing groups of
690 four, eight, and 15 male mice (**b, d**) and four, eight, and 16 female mice (**c, e**). **f-k**
691 Analysis of sex differences in CCR, comparing groups of four (**f, i**), eight (**g, j**) and
692 15/16 (**h, k**) male and female mice. **l-o** Heatmaps showing the time course of CCR over
693 2-hour intervals (**l, m**) and 12-hour intervals (**n, o**) for groups of four, eight, and 15-16
694 mice. Values in the bar or line graphs are presented as mean ± SD, with box plots
695 showing min/max whiskers. Statistical analysis was conducted using Holm-Sidak
696 method for multiple comparisons. Significance levels are indicated as *$p < 0.05$, **$p <$
697 0.01, and ***$p < 0.001$. $p < 0.001$ (**b**), $p < 0.001$ (**c**), $p = 0.882$ (**f**), $p < 0.001$ (**g**), $p <$
698 0.001 (**h**), $p = 0.873$ (**i**), $p < 0.001$ (**j**), $p < 0.001$ (**k**).
699

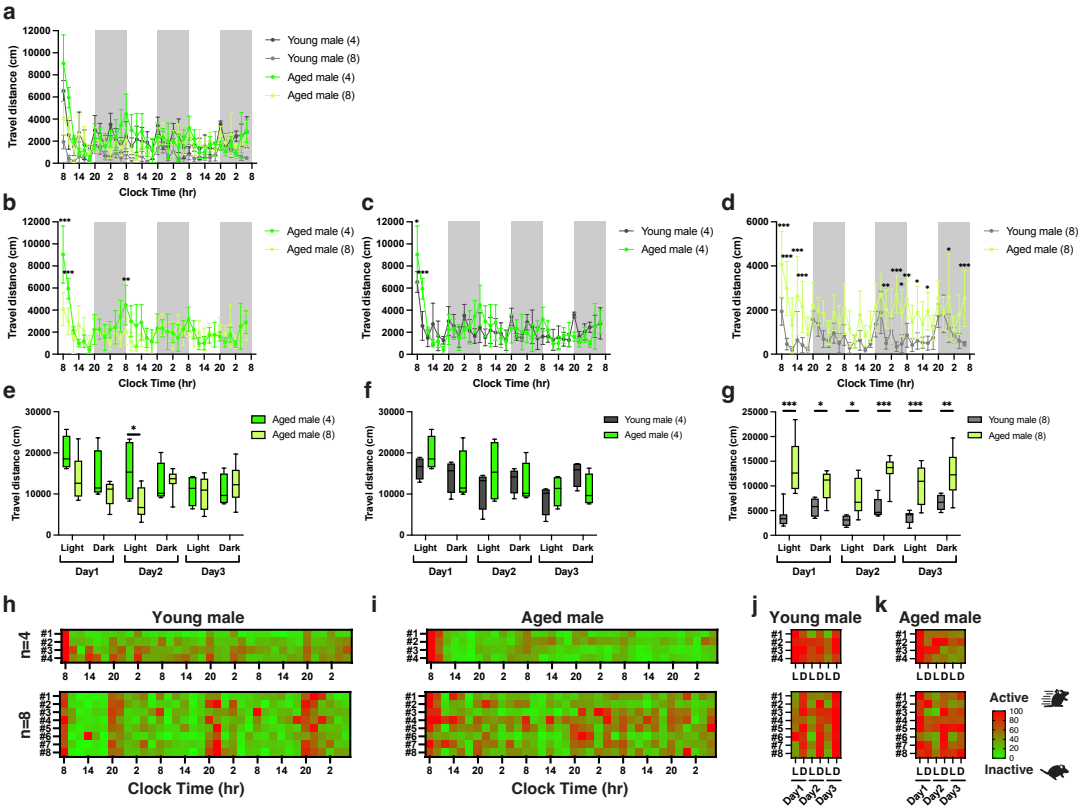

Fig. 5: Activity analysis of group-housed aged male mice using the IntelliProfiler.

a-g Cumulative travel distances measured in 2-hour intervals (**a-d**) and over 12-hour intervals (**e-g**). **b, e** Analysis of locomotor activity based on group size, comparing groups of four and eight aged mice. **c, d, f, g** Analysis of aging effects in locomotor activity, comparing groups of four young and aged male mice (**c, f**), groups of eight young and aged male mice (**d, g**). **h-k** Heatmaps showing relative locomotor activity over 2-hour intervals (**h, i**) and 12-hour intervals (**j, k**) for groups of four and eight mice. Values in the bar or line graphs are presented as mean ± SD, with box plots displaying min/max whiskers. Statistical analysis was conducted using Holm-Sidak method for multiple comparisons. Significance levels are indicated as $*p < 0.05$, $**p < 0.01$, and $***p < 0.001$. $p = 0.338$ (**c**), $p < 0.001$ (**d**), $p = 0.585$ (**f**), $p < 0.001$ (**g**).

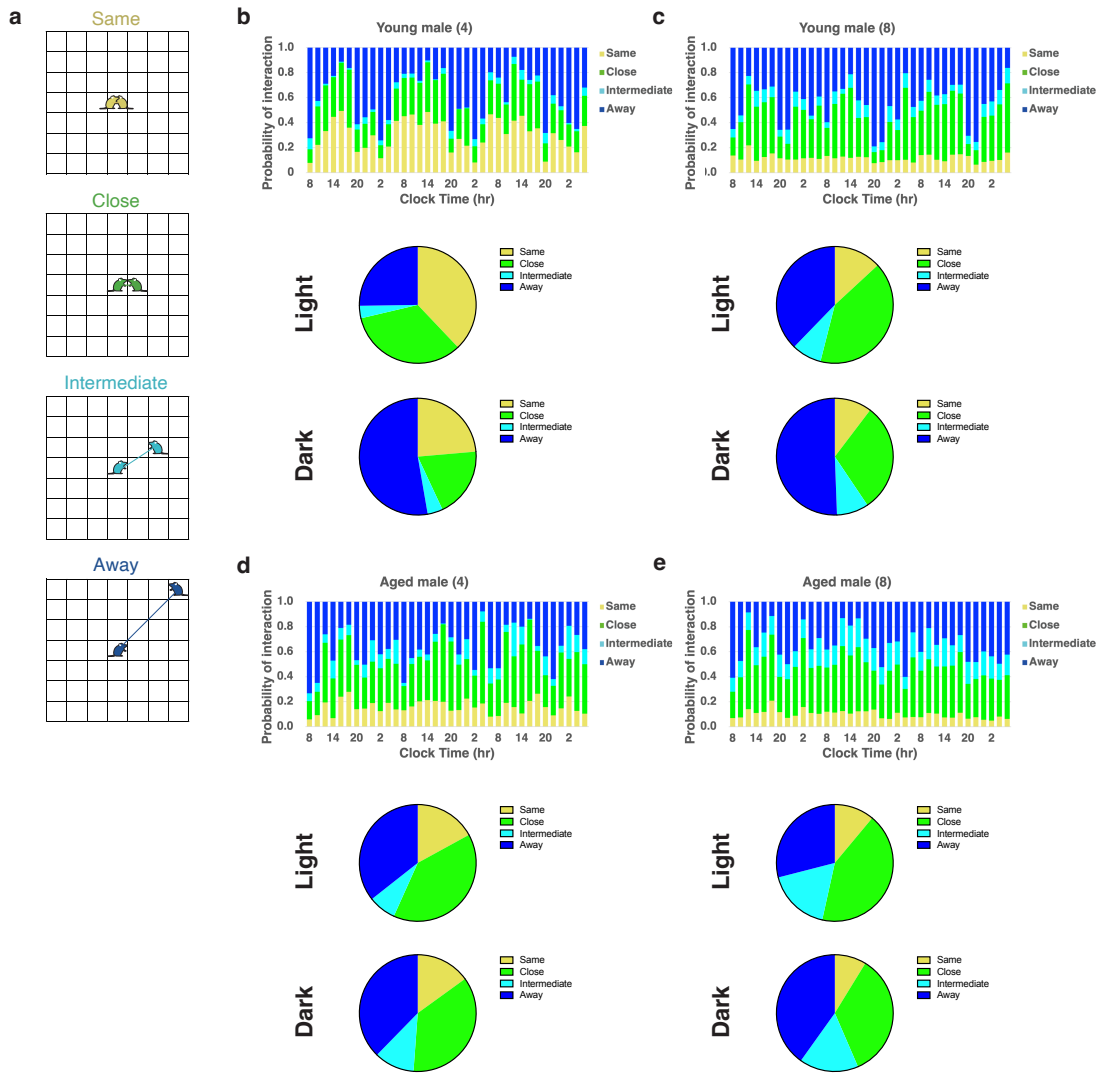

Fig. 6: The spatial relationships among group-housed aged male mice using the IntelliProfiler.

716 **a** Definition of the spatial relationships between two individual mice. When another
717 mouse is in the same grid as the focal mouse (both depicted in yellow), the relationship
718 is defined as "Same." If the other mouse is in the surrounding grids (depicted in green),
719 it is defined as "Close." If the other mouse is outside the surrounding grids (depicted in
720 light blue), it is defined as "Intermediate." If the other mouse is beyond the
721 "Intermediate" zone (depicted in blue), the relationship is categorized as "Away." **b-e**
722 The 2-hour bin transition of proportions based on "Same," "Close," "Intermediate," and
723 "Away" for groups of four young male mice (**b**), eight young male mice (**c**), four aged
724 male mice (**d**), eight aged male mice (**e**). **b-e** The average proportion of distance
725 categories during the light period and the dark period is shown for each group. Chi-
726 square p-values comparing the proportions between light and dark periods, $p < 0.001$ (**b**,
727 four young males), $p = 0.256$ (**c**, eight young males), $p = 0.836$ (**d**, four aged males), $p =$
728 0.439 (**e**, eight aged males). The p-values of chi-square for the group size, $p < 0.001$ (**b,**
729 **c**, young males in the light phase), $p = 0.020$ (**b, c**, young males in the dark phase), $p =$
730 0.115 (**d, e**, aged males in the light phase), $p = 0.477$ (**d, e**, aged males in the dark
731 phase).
732

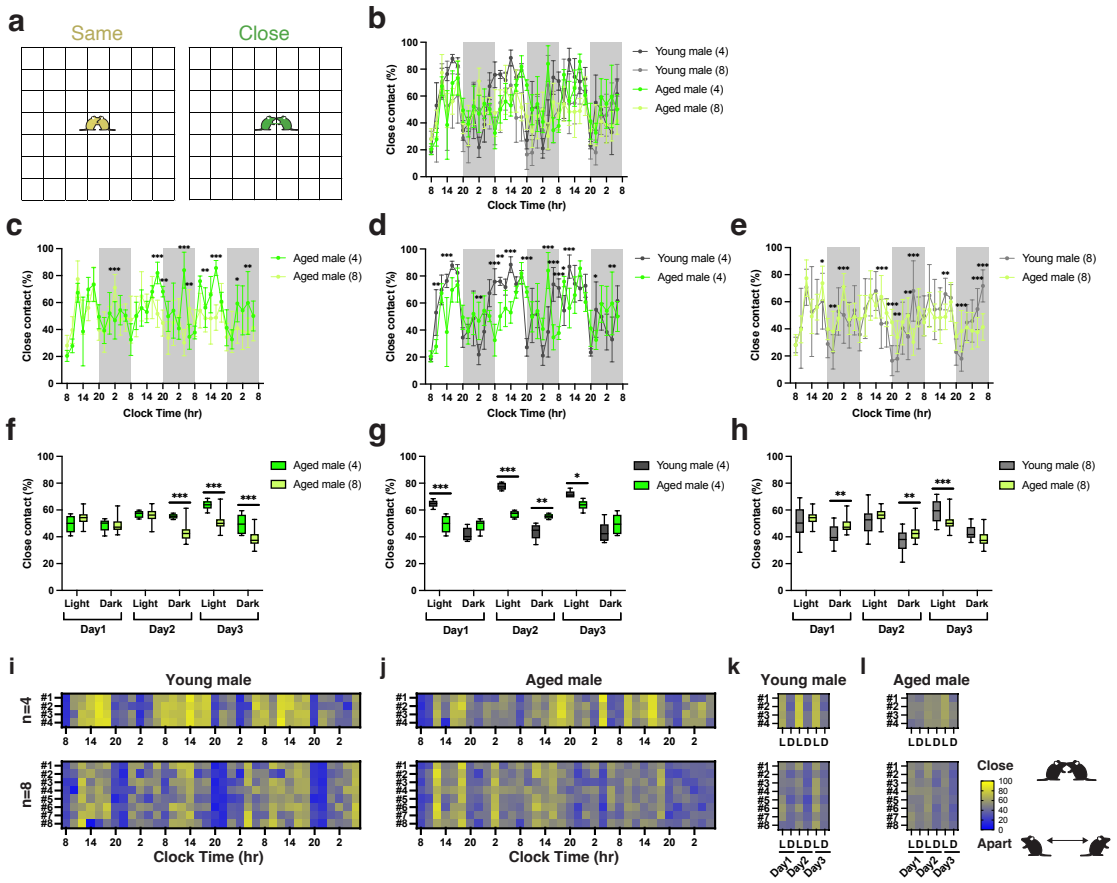

Fig. 7: Close contact between two individuals among group-housed aged male mice analyzed using the IntelliProfiler.

a Definition of close contact, where two mice either in either "Same" (depicted in yellow) or in adjacent grids, classified as "Close" (depicted in green). **b-h** Average Close Contact Ratio (CCR) measured in 2-hour intervals (**b-e**) and 12-hour intervals (**f-h**). **c, f** Analysis of CCR based on group size, comparing groups of four and eight young and aged males. **d, e, g, h** Analysis of CCR based on aging effects, comparing groups of four young and aged male mice (**d, g**), groups of eight young and aged male mice (**e, h**). **i-l** Heatmaps showing the time course of CCR over 2-hour intervals (**i, j**) and 12-hour intervals (**k, l**) for groups of four and eight mice. Values in the bar or line graphs are presented as mean ± SD, with box plot showing min/max whiskers. Statistical analysis was conducted using Holm-Sidak method for multiple comparisons. Significance levels are indicated as $*p < 0.05$, $**p < 0.01$, and $***p < 0.001$. $p < 0.001$ (**c**), $p = 0.338$ (**d**), $p = 0.072$ (**e**), $p < 0.001$ (**f**), $p = 0.007$ (**g**), $p = 0.109$ (**h**).

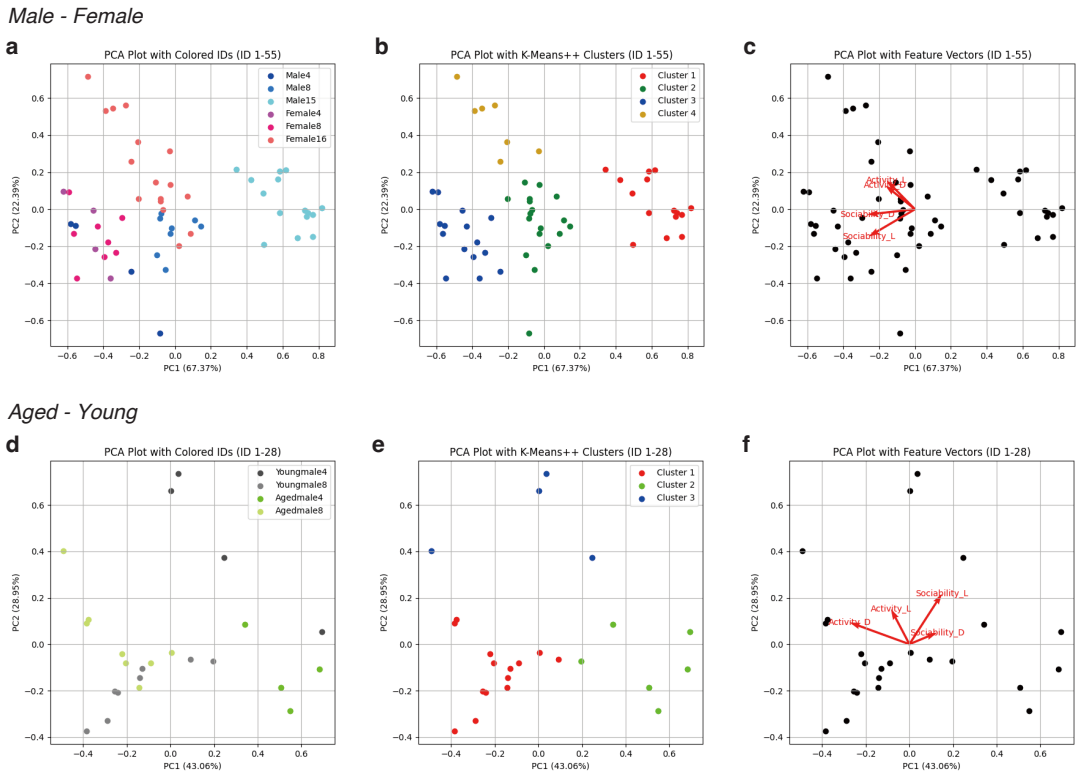

Fig. 8: Principal component analysis of group behavior using the IntelliProfiler.

751 **a-f** Principal component analysis (PCA) of group behavior in four, eight, and 15/16

752 male and female mice (**a-c**) and in young and aged mice in groups of four and eight (**d-**

753 **f**). **b, e** K-means clustering in PCA plots. **c, f** Analysis of feature vectors, focusing on

754 Close Contact Ratio (CCR) and relative activity during the light and dark periods.

755

756

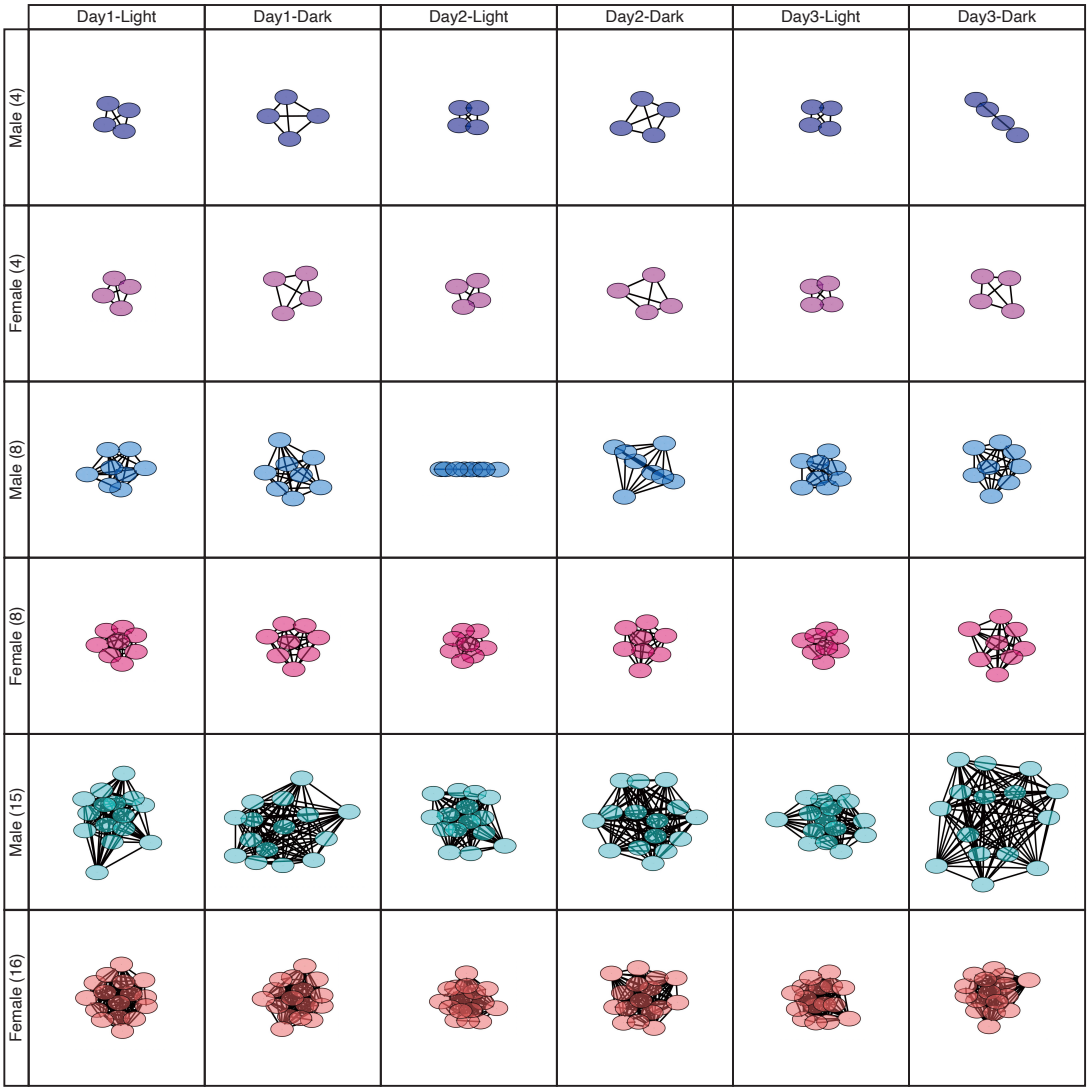

Fig. 9: Network analysis of social interaction in the male and female mice using the IntelliProfiler.

Network analysis of social interactions during the light period on day 1 and the dark period on day 3 in groups of four, eight, and 15/16 male and female mice. Nodes represents individual mice, and edges reflects the relative social contacts between two individuals. The network graph was generated using Cytoscape. Supplementary Fig. 4 provides additional network diagrams, where unique color code for each individual highlight the individual-specific social dynamics within the network.

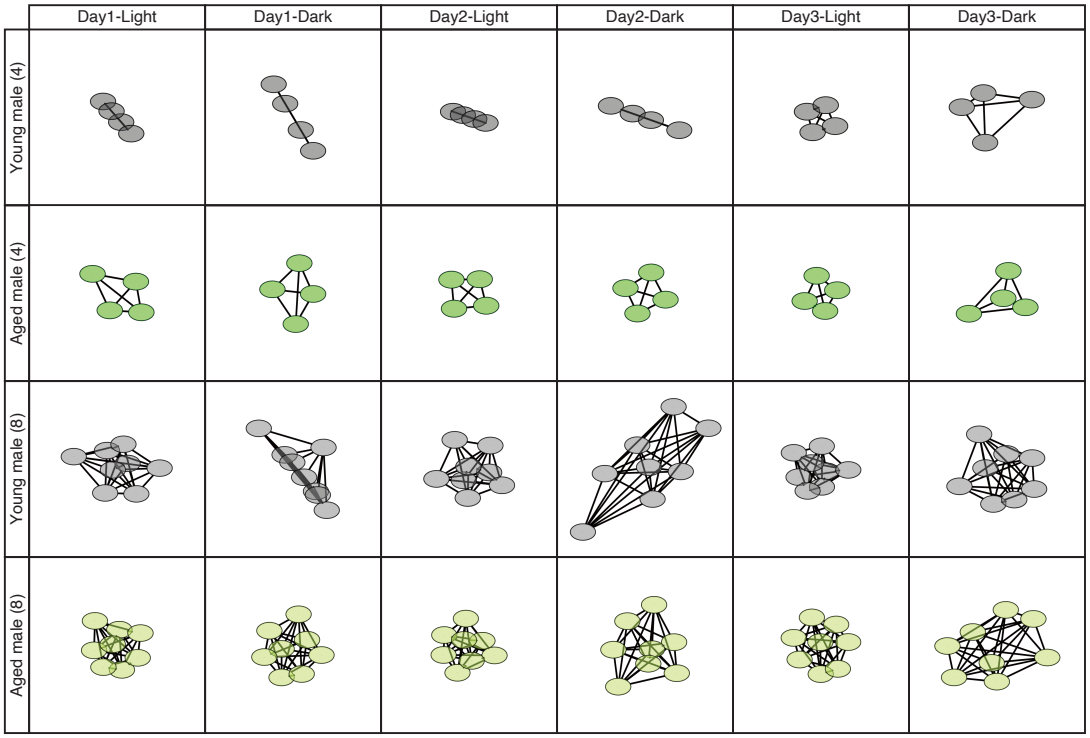

Fig. 10: Network analysis of group interaction in young and aged male mice using the IntelliProfiler.

771 Network analysis of social interactions during the light period on day 1 and the dark

772 period on day 3 in groups of four and eight young and aged males. Each circle

773 represents an individual mouse, and the proximity of the lines indicates the relative

774 social distance between two individuals. The network graph was generated using

775 Cytoscape. Supplementary Fig. 5 provides further details, offering a clear understanding

776 of individual-specific social dynamics across the networks.